

Interplay of quantum spin Hall effect and spontaneous time-reversal symmetry breaking in electron-hole bilayers: Zero-field topological superconductivity

T. Paul¹, V. F. Becerra¹, and T. Hyart^{1,2}

¹International Research Center MagTop, IFPAN, Warsaw, Poland

² Department of Applied Physics, Aalto University, Espoo, Finland

tpaul@magtop.ifpan.edu.pl, arXiv.2205.13348

TAKE HOME MESSAGE

Utilizing excitons to break spontaneous time reversal symmetry and to realize Majorana zero modes without using magnetic field or ferromagnetic insulators

INTRODUCTION

It has been proposed that in band-inverted electron-hole bilayers the excitonic correlations arising due to Coulomb interactions lead to phase transitions from a trivial insulator phase to an insulating phase with spontaneously broken time reversal symmetry (TRS) and finally to a nontrivial quantum spin Hall (QSH) insulator phase as a function of reversing electron and hole densities [1, 2].

$$H_0 = \left(\frac{\hbar^2 k^2}{2m} - E_G \right) \tau_z \sigma_0 + A k_x \tau_x \sigma_z - A k_y \tau_y \sigma_0 + \Delta_z \tau_y \sigma_y, \quad (1)$$

$$H_{EC} = \Re[\Delta_1] \tau_y \sigma_y + \Re[\Delta_2] [k_x \tau_x \sigma_z - k_y \tau_y \sigma_0] + \Im[\Delta_1] \tau_x \sigma_y - \Im[\Delta_2] [k_x \tau_x \sigma_z + k_y \tau_y \sigma_0], \quad (2)$$

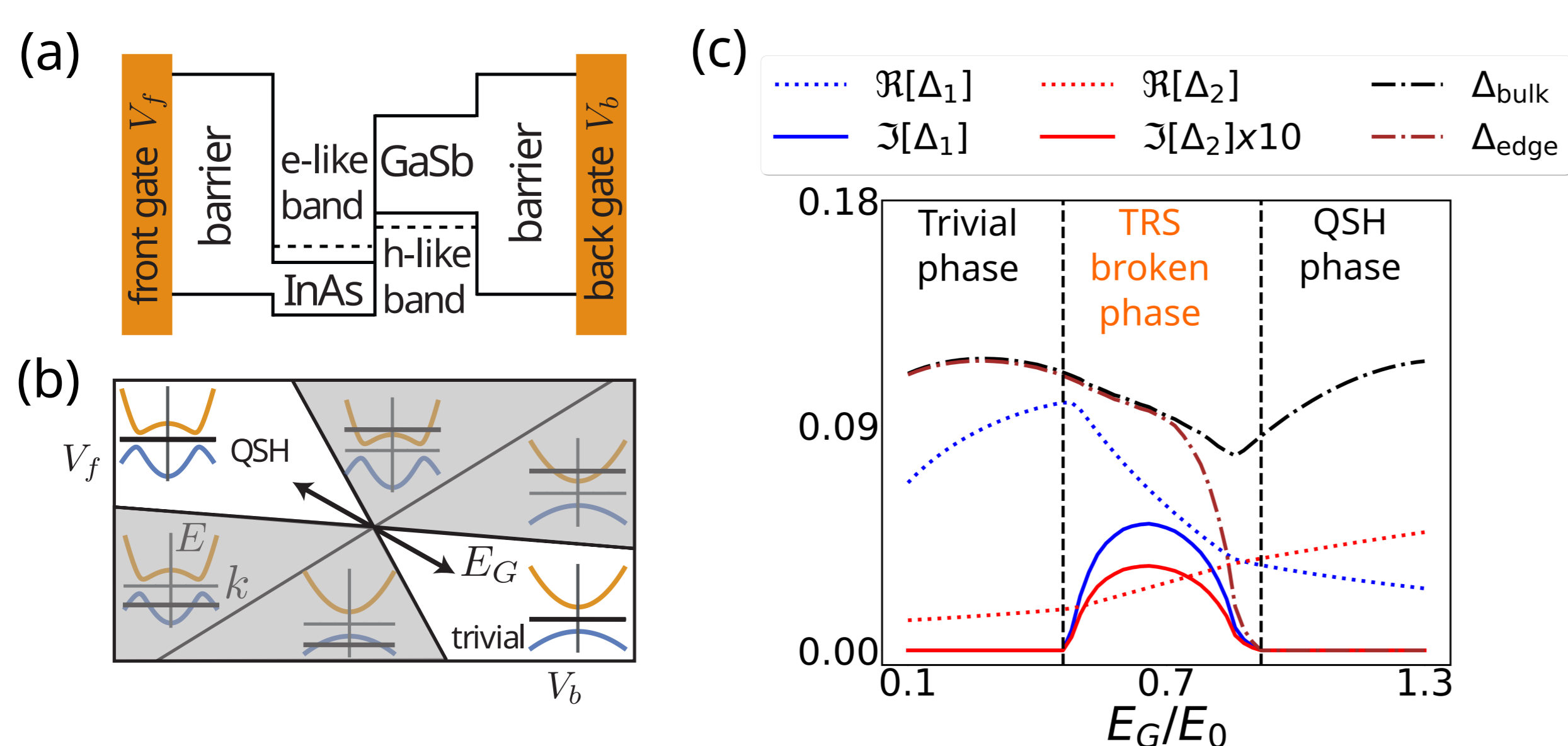


Figure 1: (a) Schematic set-up to control hole and electron densities via gate voltages. (b) Topological phase diagram as function of gate voltages. (c) Topological phase diagram as a function of E_G . In the TRS broken phase $\Im[\Delta_1], \Im[\Delta_2] \neq 0$. [2]

EFFECTIVE EDGE THEORY

To investigate the edge excitations in the presence of induced superconductivity and time-reversal symmetry breaking order parameter, we develop an effective edge theory which is valid for energies smaller than the bulk gap, $|E| \ll \Delta_{\text{bulk}}$:

$$H_e = \begin{pmatrix} A_{\text{eff}}(x)k_x & -i\Delta_{\text{ex}}(x) & \Delta_s(x) & 0 \\ i\Delta_{\text{ex}}(x) & -A_{\text{eff}}(x)k_x & 0 & \Delta_s(x) \\ \Delta_s^*(x) & 0 & -A_{\text{eff}}(x)k_x & -i\Delta_{\text{ex}}(x) \\ 0 & \Delta_s^*(x) & i\Delta_{\text{ex}}(x) & A_{\text{eff}}(x)k_x \end{pmatrix}, \quad (3)$$

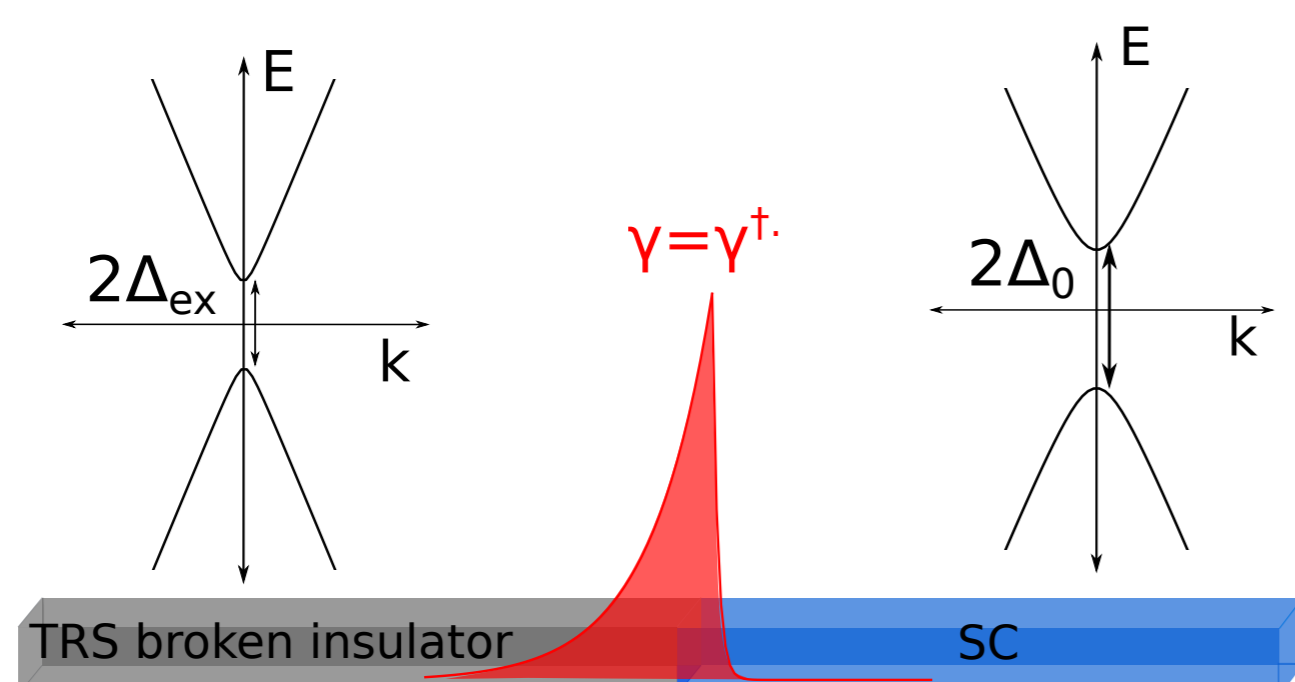


Figure 2: Schematic illustration of a Majorana zero mode (MZM) found at $x=0$ (in red) when TRS broken phase (superconductor) covers the region $x < 0$ ($x > 0$) [3].

ZERO FIELD TOPOLOGICAL SUPERCONDUCTIVITY

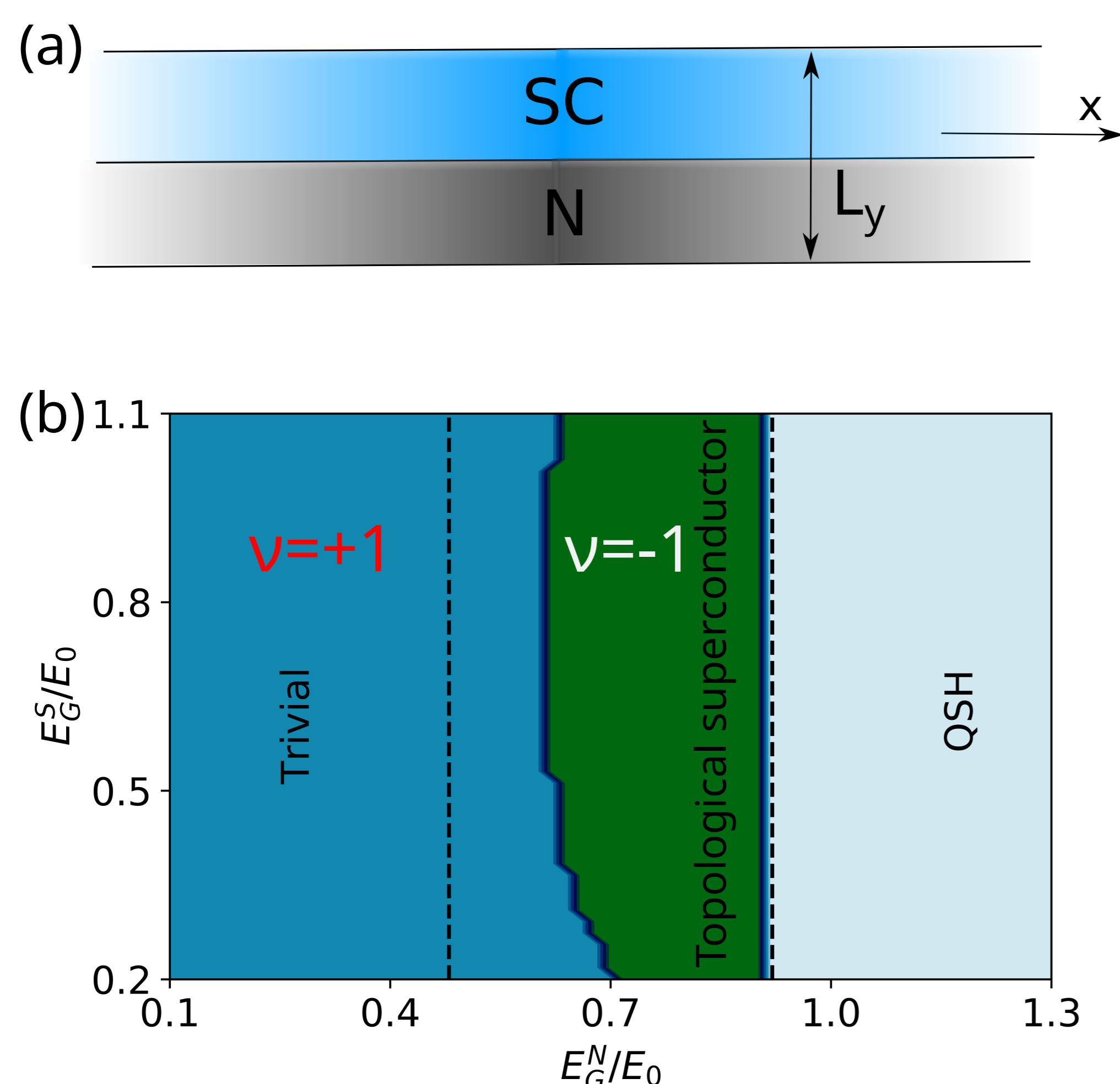


Figure 3: (a) Schematic set-up to compute the \mathbb{Z}_2 invariant. (b) Topological phase diagram as a function of E_G^S and E_G^N . In the trivial phase, the hybrid system does not support MZMs. In the topologically nontrivial phase, the system supports MZMs at the interface of the TRS broken insulator and superconducting regions. [3].

DETECTION OF MZMs: 4π JOSEPHSON CURRENT

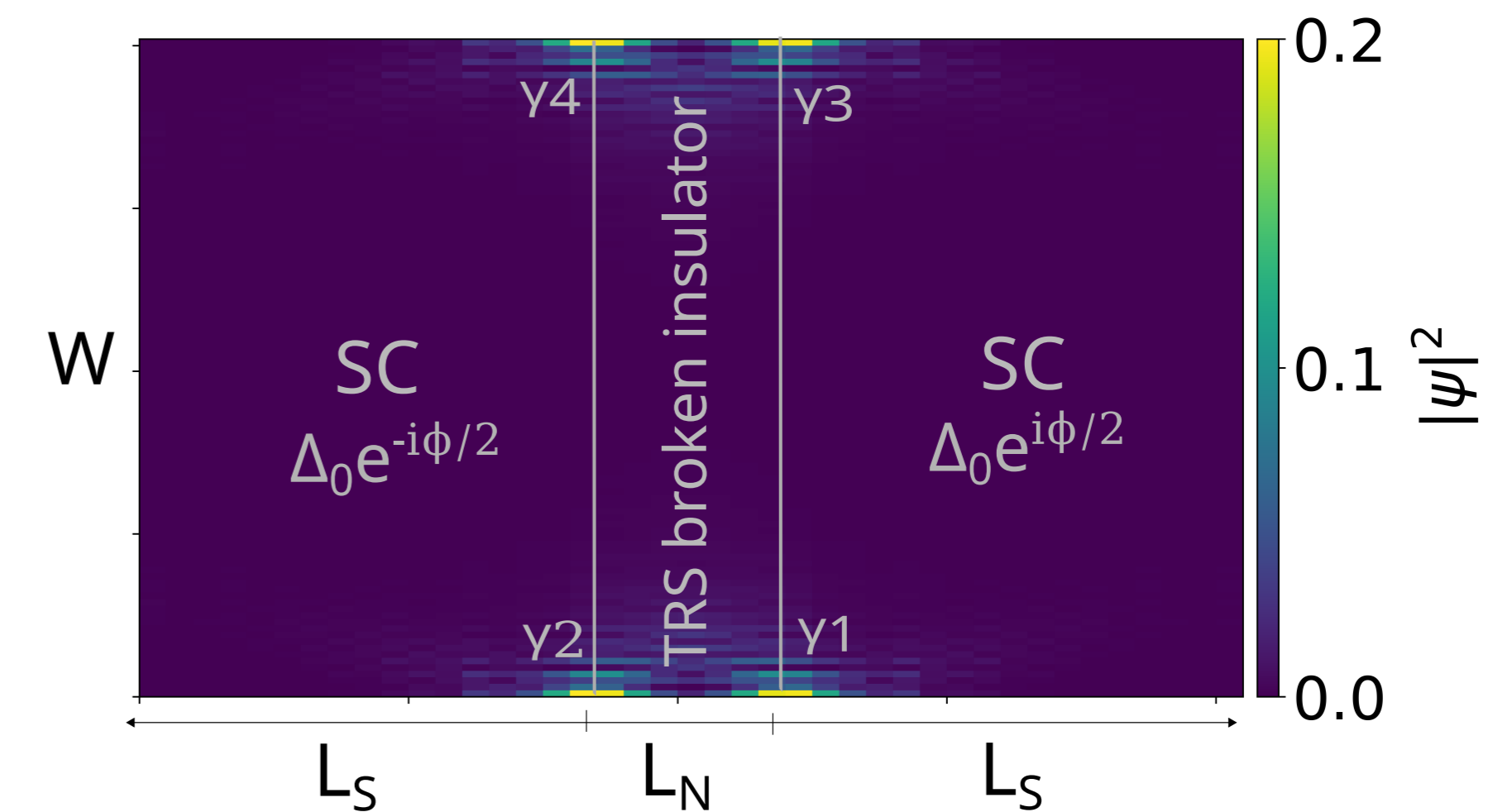


Figure 4: Superconductor/TRS broken insulator/ superconductor Josephson junction (JJ) for detection of the MZMs via the 4π Josephson effect. The system supports two MZMs γ_1 and γ_2 (γ_3 and γ_4) on the bottom (top) edge as shown in the local density of states with the colors [3].

The Josephson-current is given by:

$$I(\phi) = I_{2\pi} \sin(\phi) + I_{4\pi} \frac{\mathcal{P}_{12} + \mathcal{P}_{34}}{2} \sin(\phi/2) + h.h., \quad (4)$$

where $\mathcal{P}_{12} = i\gamma_1\gamma_2$ and $\mathcal{P}_{34} = i\gamma_3\gamma_4$.

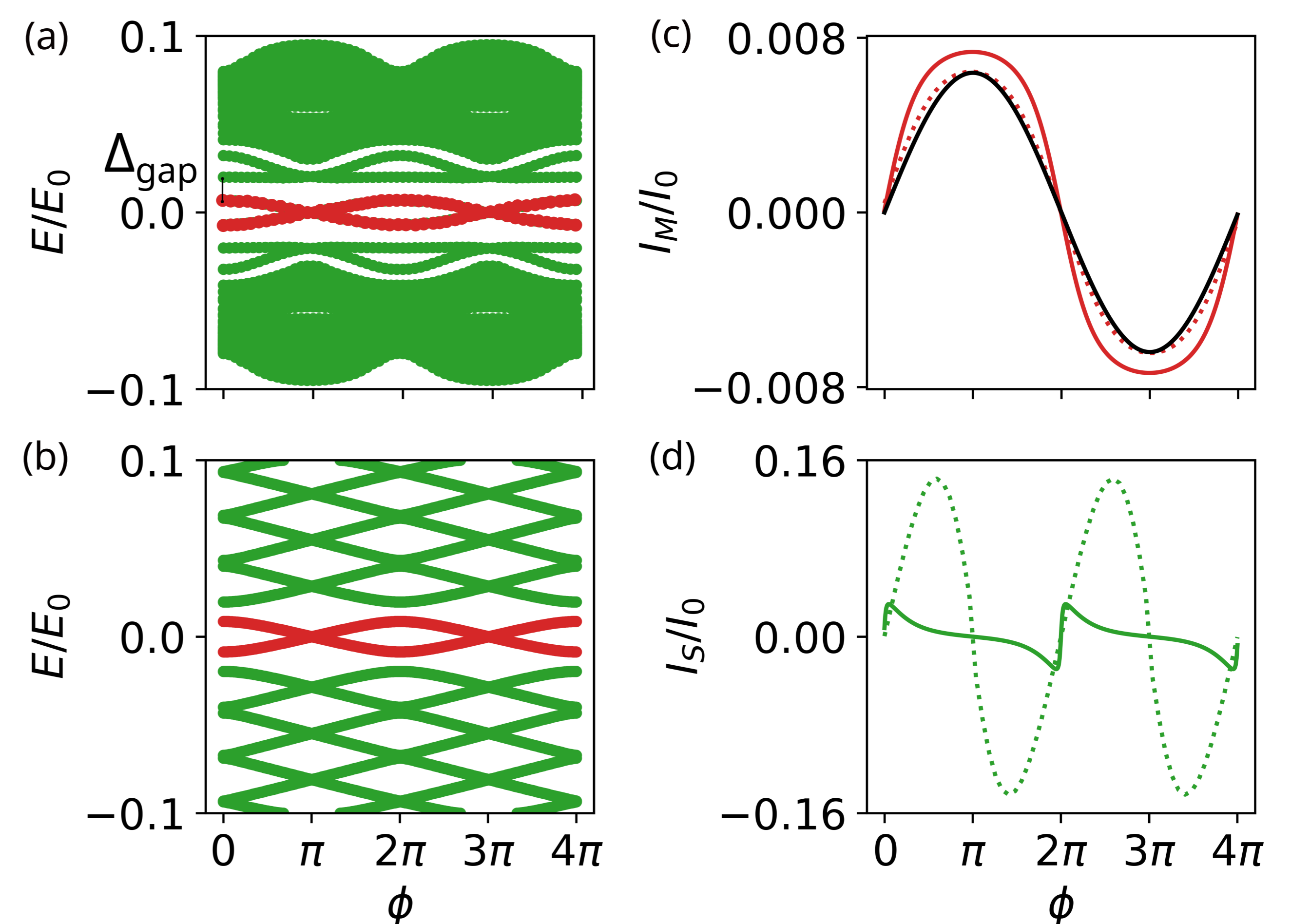


Figure 5: Spectrum of JJ as a function of phase bias ϕ for $\nu = -1$ obtained (a) Numerically obtained from the full tight binding model (b) using the effective edge theory. Comparison of magnitude of (c) 4π - (d) 2π - Josephson current obtained from numerics (dotted) and effective edge theory (solid). The black line in (c) corresponds to the 4π current obtained from the effective edge theory in the asymptotic limit $I_{4\pi} = \frac{2e}{\hbar} \frac{\Delta_0 \Delta_{\text{ex}}}{\Delta_0 + \Delta_{\text{ex}}} e^{-\Delta_{\text{ex}} L_N / A_{\text{eff}}^N}$ [3].

THEORETICAL CONDITIONS TO OBSERVE MZMs

- ✓ MZMs at the opposite edge states are not coupled to preserve parity.
- ✓ Josephson frequencies ($f_{2\pi} = 2eV/h$, $f_{4\pi} = eV/h$) are much larger than quasiparticle poisoning rate (1Hz to 10 MHz).
- ✓ No Landau Zener tunneling or thermally excited quasiparticles: $\hbar f_{2\pi}, \hbar f_{4\pi}, k_B T$ are smaller than Δ_{gap}/E_0 .
- ✓ $I_{4\pi}$ should be sufficiently large to overcome detector sensitivity
- ✓ $I_{2\pi}$ peak should not overshadow $I_{4\pi}$ peak.

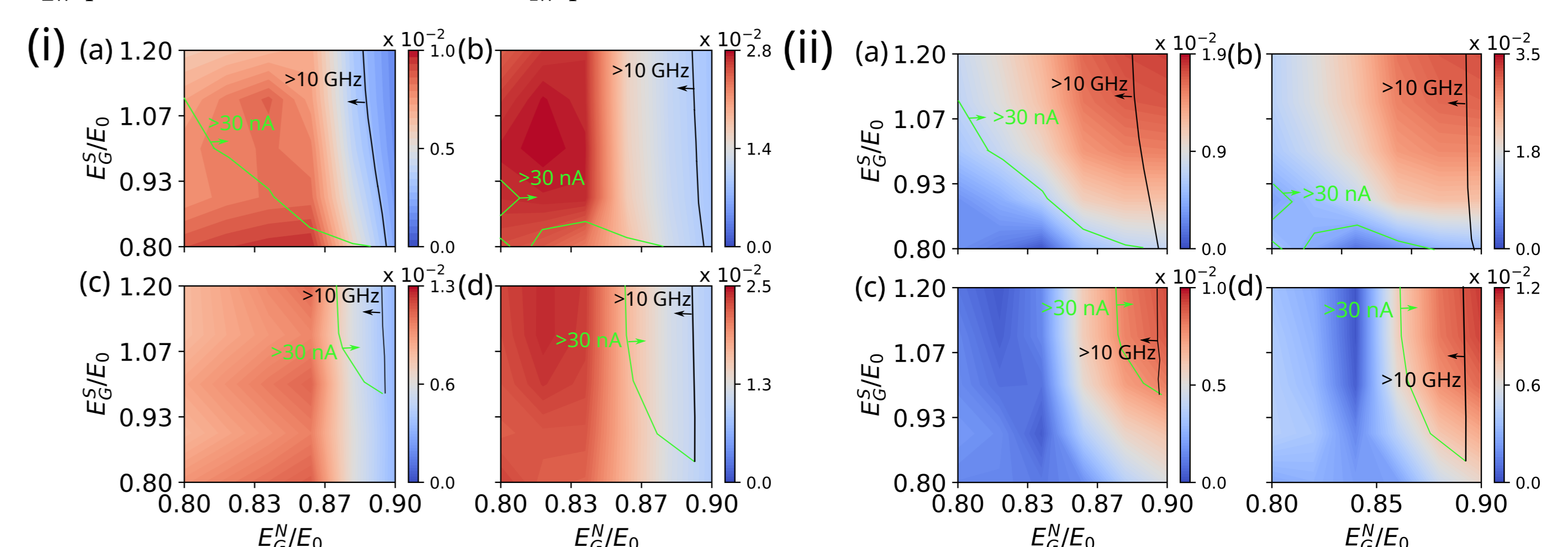


Figure 6: (i) Energy gap Δ_{gap}/E_0 between the MZMs and the other Andreev levels and (ii) $I_{4\pi}/I_0$ as a function of E_G^N and E_G^S for different combinations of L_N and Δ_0 values. The optimal parameter regimes for the observation of the 4π Josephson effect is the region between black and green lines. [3].

References

- [1] D. I. Pikulin and T. Hyart. Interplay of exciton condensation and the quantum spin hall effect in InAs/GaSb bilayers. *Phys. Rev. Lett.*, 112:176403, Apr 2014.
- [2] Tania Paul, V. Fernández Becerra, and Timo Hyart. Interplay of quantum spin Hall effect and spontaneous time-reversal symmetry breaking in electron-hole bilayers I: Transport properties. arXiv.2205.12790.
- [3] Tania Paul, V. Fernández Becerra, and Timo Hyart. Interplay of quantum spin Hall effect and spontaneous time-reversal symmetry breaking in electron-hole bilayers II: Zero-field topological superconductivity. arXiv.2205.13348.